RSC Advances

ROYAL SOCIETY OF CHEMISTRY

www.rsc.org/advances

RSC Advances

RSCPublishing

ARTICLE

Design of oligoaziridine-PEG coatings for efficient nanogold cellular biotagging

Cite this: DOI: 10.1039/xoxxoooooox

A. Sofia Silva,[a,b] Vasco D. B. Bonifácio,[a,c,*] Vivek P. Raje,[a] Paula S. Branco,[a] Paulo F.B. Machado,[b] Ilídio J. Correia,[b] and Ana Aguiar-Ricardo,[a,*]

Received ooth January 2012,
Accepted ooth January 2012

DOI: 10.1039/xoxxoooooox

www.rsc.org/

Gold nanoparticles (AuNPs) are the most investigated nanomaterials for theragnosis applications. In a research field where live cell assays, as well as the tracking of nanomaterials into cell's environment, are of extremely importance, water-soluble AuNPs have been intensively studied to overcome the toxic effects exerted by coatings. Unfortunately, AuNPs fluorescent tagging often fails due to self-quenching and a careful design must be carried out to keep optoelectronic properties and biocompatibility. In this work, the synthesis of fluorescent gold nanoprobes, able to enter within cell's environment (biotags) and target the cell nucleus, was designed and the particles tracked by confocal laser scanning microscopy. The coating of AuNPs with maleimide poly(ethylene glycol) and fluorescent oligoaziridine biocompatible oligomers, resulted in robust, optical active biotags that open novel insights into cancer theragnosis.

1. Introduction

Cellular internalization and nuclear targeting are two subsequent and challenging tasks that have been increasingly investigated over the past decades. The cell nucleus is the place where the genetic information and transcription machinery of the cell can be encountered and, therefore, its targeting has been demonstrated to be crucial for several diagnostic and therapeutic purposes.[1] In such targeting attempts, different types of nanoparticles (metallic, magnetic or polymeric) have been introduced into the cells environment.[2–9] Particularly, gold nanoparticles (AuNPs) have been widely in the field of nanomedicine for theranostic aspirations. These nanomaterials display interesting optical, electronic, and molecular-recognition properties not shown by bulk gold.[10–13] They are easily reproducible in a wide variety of shapes and sizes, and can be functionalized to perform specific functions, through the attachment of biologically active molecules, targeting sequences, imaging devices and biocompatible coatings.[14,15]
The targeting of fluorescent agents to cells and tissues by using AuNPs has emerged as a main focus in cancer research since nonspecific toxicity can be minimized and transportation efficiency can be enhanced.[16–20] However, AuNPs are well known to self-quench upon surface fluorescent tagging. Notwithstanding, under certain conditions, the fluorescence can be enhanced by the near-field of AuNPs, which is a subject of considerable interest.[21,2223] Aiming the development of robust gold biotags, able to target the cells environment, and ultimately the nucleus, we investigated novel biocompatible coatings comprising oligomers of PEG and a fluorescent water-soluble oligoaziridine (OA). Although OA, was already investigated as a biosensor for fluorescence microscopic imaging of metal cations under physiological conditions,[24] we now demonstrate its efficient biotagging performance. To foster internalization features, while guarantying nanoparticle stability and avoiding unspecific interactions, a biocompatible coating based on homobifunctional maleimide poly(ethylene glycol) (MPM) units was chosen. The selection of MPM relied mainly on its biocompatibility and high reactivity.[25–28]
Using a convergent strategy we were able to synthesize stable PEG-oligoaziridine fluorescent water-soluble bilayered AuNPs through a simple and straightforward route. The cellular uptake of these novel gold nanoparticles was followed through fluorescence microscopy and their biocompatible profile was assured through the MTS assay. Morphological and spectral characterizations were also performed.

2. Results and Discussion

2.1 Particles synthesis and characterization

The particle design aimed the construction of bilayered, biocompatible and optical active gold nanoparticles. The first layer (PEG oligomer) was assembled into the AuNPs by the reaction of the alcohol from citrate with the MAL-PEG-MAL homobifunctional oligomer (Au-MPM). The reaction of alcohols with maleimide is reported in the presence of a catalytic amount of Au^{3+},[29] and the successful AuNPs

PEGylation led us to conclude that indeed AuNPs (synthesized using a Au^{3+} precursor), must be involved in this step. Next, a second layer (OA fluorescent oligomer) was added by reacting OA with the terminal maleimide from Au-MPM (Au-MPM-OA). Following this strategy (see schematic synthesis in Fig. 1) we were able to synthesize stable nanogold biotags avoiding elaborated synthesis and purification.

The MPM coating was confirmed by FT-IR through the presence of the characteristic (slightly shifted) ether bands (1552, 1296, and 1137 cm^{-1}) (Fig. 1A). Similarly, the OA coating was confirmed by the presence of sulfonamide bands (1658, 1362 and 1156 cm^{-1}) (Fig. 1B). As expected, in the final formulation Au-MPM-OA, both bands from MPM and OA were identified (1650, 1362 and 1148 cm^{-1}), thus proofing the successful reaction between Au-MPM and OA.

After the synthesis different nanogold formulations were developed. The influence of OA (fluorescent biosensor) and PEG oligomers on the particles morphology and size was investigated using different molar ratios of OA and MPM (100:1, 500:1, 750:1, 1250:1, 2500:1, 5000:1, 10000:1),[30] leading to the production of Au-OA, Au-MPM and Au-MPM-OA formulations.

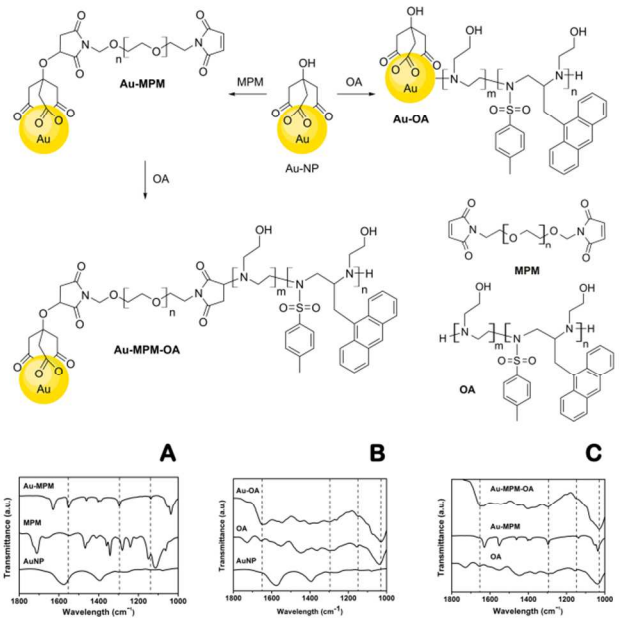

Fig. 1 PEG-oligoaziridine bilayer coating of gold nanoparticles: schematic synthesis (top) and the corresponding IR spectra (bottom) of Au-MPM (A), Au-OA (B) and Au-MPM-OA (C).

The nanoparticles morphology was assessed by Transmission Electron Microscopy (TEM). We found that the best molar ratios for OA:AuNPs and MPM:AuNPs were 750:1 and 5000:1, respectively. The produced biotags showed spherical and oval-like morphologies as it can be observed in Fig. 2.

The nanoparticles were also characterized in terms of their ability to form stable colloidal formulations with appropriate physicochemical properties for intracellular applications.

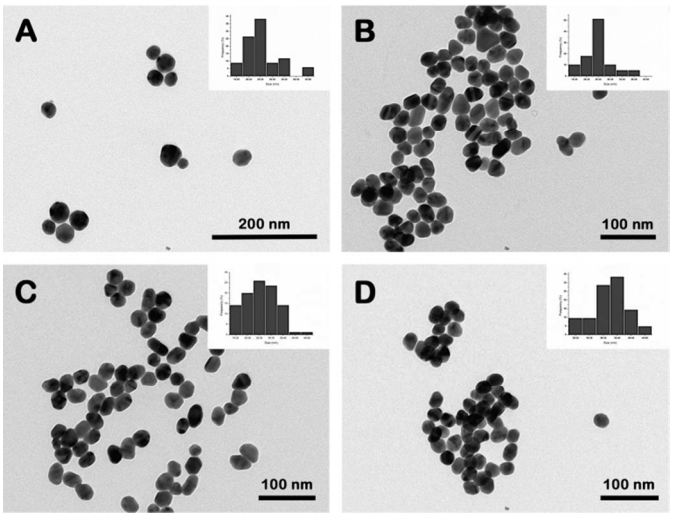

Fig. 2 TEM images of the biotags: (A) gold nanoparticles, (B) gold nanoparticles coated with oligoaziridine (Au-OA), (C) gold nanoparticles coated with MPM (Au-MPM) and (D) PEGylated gold nanoparticles coated with oligoaziridine (Au-MPM-OA). The insets show size measurements performed using the Image J software.

Dynamic light scattering (DLS) was also performed to evaluate the nanoparticles size, and similar values were obtained using both methods. All formulations exhibited sizes well-suited for delivery into tumoral microenvironments. As expected, the AuNPs show sizes around 30 nm and a zeta potential of approximately -30 mV [18,31] (see Fig. 2A and Table 1). After coating with OA, the zeta potential tends to became positive, thus favoring cellular internalization due to electrostatic interaction between negatively charged proteoglycans and positively charged nanoparticles.[32] Our data showed that all the produced formulations have positive zeta potential values within the range of colloidal stability (between -40 to +40 mV).

Table 1 Particle size and zeta potential data for nanogold PEG-oligoaziridine coatings

Nanoparticles	Particle size (nm)	PDI	Zeta potential (mV)
AuNP	28±1	0.369	-34±4
Au-OA[a]	30.7±0.5	0.371	18±1
Au-MPM[a]	28.4	0.379	-31±4
Au-MPM-OA[b]	28±1.5	0.396	20.4±2

[a]Au-MPM/OA biosensor 5000:1 ratio;[b]Au-MPM/OA biosensor 750:1 ratio.

The amount of organic components on the AuNPs was assessed by thermal gravimetric analysis (TGA) (see Fig. ESI 1 in the Electronic Supporting Information). The total mass loss was 6.67%, 6.11% and 4% for Au-MPM, Au-OA and Au-MPM-OA, respectively. By combining the data from TGA and inductively coupled plasma (ICP) analyses, the amount of Au and S in the nanoparticles was determined (see calculations in Electronic Supporting Information), thus confirming a bilayered architecture (MPM/OA 1:1 ratio).

The synthesized bilayered nanogolds showed a high colloidal stability that was corroborated by UV-Visible spectroscopy (Fig. 3A) and by colorimetric analyses (Fig. 3B). By comparing the absorbance intensity of the characteristic band of AuNPs

(spectrum 1 in Fig. 3A, λmax= 526 nm) of the formulations, we found that all coatings lower the intensity of this band (more significantly in case of Au-OA, spectrum 3 in Fig. 3A). However, for the formulation Au-MPM-OA (750:1 ratio) the intensity is recovered (spectrum 8 in Fig. 3A), demonstrating a synergistic effect between MPM and OA layers. For higher ratios (1250:1 and 2500:1) the variation in the absorption is negligible.

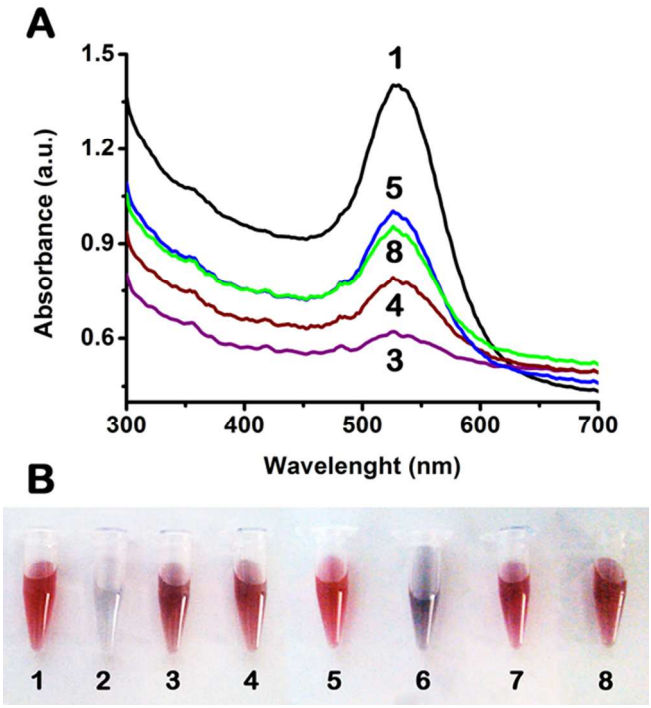

Fig. 3 Colloidal stability of the biotags: (A) UV-Vis spectra and (B) colorimetric evaluation: (1) AuNPs, (2) Au-OA 2500:1, (3) Au-OA 1250:1, (4) Au-OA 750:1, (5) Au-MPM, (6) Au-MPM-OA 2500:1, (7) Au-MPM-OA 1250:1, (8) Au-MPM-OA 750:1.

The optical properties of the biotags were evaluated in aqueous media. Interestingly, biotags coating with OA leads to optical active nanoparticles, thus avoiding self-quenching events (Figure ESI 2, Electronic Supporting Information).

3.2 Qualitative evaluation of biotags cellular uptake

In the present study, the A549 cell line was used as a model to study the cellular uptake of the OA biosensor, Au-OA and Au-MPM-OA nanogold formulations. Also an evaluation of the produced biotags was performed to conclude about their suitability for cell live imaging applications using microscopic fluorescence. Fluorescence (Fig. 4) and Confocal Laser Scanning Microscopy (CLSM) images (Fig. 5) gave insights on cell internalization, without requiring any auxiliary reagents to 'force' their entry. The fluorescence images show that the OA biosensor (Fig. 4A), as well as the synthesized nanogolds, Au-OA (Fig. 4B) and Au-MPM-OA (Fig. 4C), were able to enter into the cells environment. It should be stressed out that all of the images regarding internalization studies were taken with the same color ranges and contrast features.

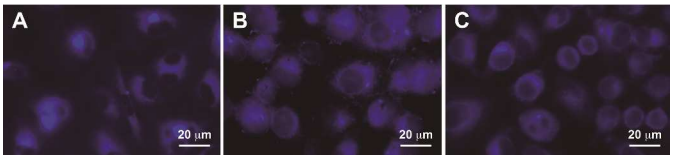

Fig. 4 Fluorescence images of A549 cells transfected with (A) an oligoaziridine biosensor, (B) Au-OA and (C) Au-MPM-OA biotags. Original magnification x63.

CLSM images showing intracellular localization of Au-OA and Au-MPM-OA are displayed in Fig. 5A and 5B, respectively.

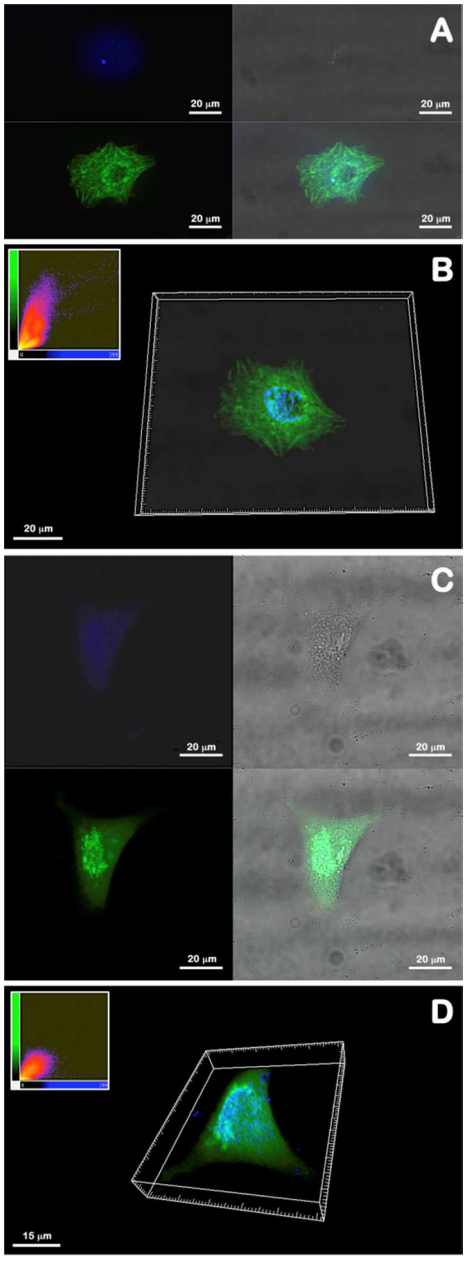

Fig. 5 Cellular uptake of the biotags: CLSM images of A549 cells transfected with (A) Au-OA and the respective 3D reconstruction (B); (C) A549 cells transfected with Au-MPM-OA and the respective 3D reconstruction (D). Green color – CellLight® Actin-GFP, BacMam 2.0; Blue color – GNP. Original magnification x40. Figures 5B and 5D were further processed using the Imaris Bitplane software.

These images show that biotags are located both within cell cytoplasm and nucleus, clearly demonstrating their potential application as imaging agent and/or as drug delivery agents when loaded with anti-cancer drugs. The high cellular internalization verified for both nanogold formulations can be easily rationalized from their physico-chemical properties such as size, zeta potential, morphology and hydrophobicity. When comparing the cellular uptake of the different nanogold formulations, we noticed that Au-MPM-OA exhibits a slightly higher internalization (Fig. 5B and 5D), a finding that was also corroborated by the analysis of *Image J* color histograms of the cell region (the artifacts/particles outside the cells were not taken into account, see Fig. ESI 3 in the Electronic Supporting Information). Co-localization histograms represented in Fig. 5B and 5D also show a higher amount of co-localized pixels for Au-MPM-OA particles. In fact, PEGylation is known to enhance materials integration within biological systems.[2,33] Thus, Au-MPM-OA are more likely to be uptaken by cancer cells.

3.3. Evaluation of the cytotoxic profile of the biotags

The cytotoxic profile was assessed after the cellular uptake took place. The MTS assay showed that cells in contact with the biotags showed higher cell viability than the positive control (K+) (ethanol) but lower than that of the negative control (K-) (culture medium), during the period of incubation (48 h). Although in literature there are different studies reporting contradictory results regarding AuNPs cytotoxicity,[15,34] we found that the biotag precursors, as well as the gold nanoparticles per se, did not affect cell viability, being above 80% for all samples. Besides, a significant difference in cell viability was obtained between the positive and negative control ($p < 0.05$), and cells exposed to the different precursors and biotags after 24 h ($p^* < 0.05$) and 48 h ($p\# < 0.05$) of incubation (Fig 6). Cell growth and adherence of the cells with internalized nanoparticles was also observed in the inverted microscopy micrographs (see Fig. ESI 4 in Electronic Supporting Information).

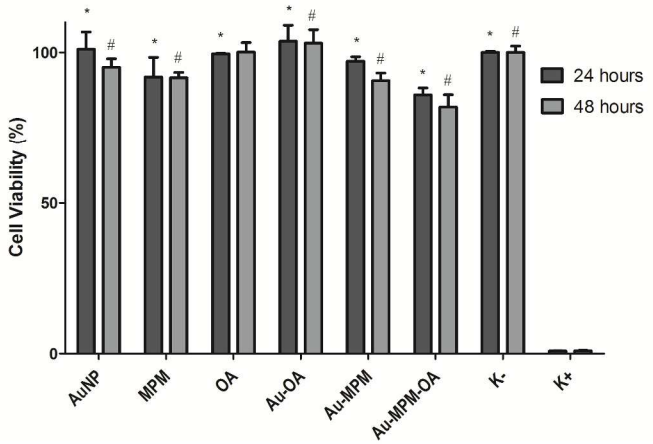

Fig. 6 Cellular activities measured by the MTS assay after 24 h and 48 h in contact with the biotags and respective precursors. MPM= MAL-PEG-MAL; OA= Oligoaziridine biosensor (OA). Negative control (K-); Positive control (K+).

Conclusions

Gold nanoparticles coated with a PEG-oligoaziridine bilayer were fully investigated and found to be stable, biocompatible, optical active and water-soluble biotags, able to target the cell nucleus. Live cell assays were assured in a faster, accessible and precise manner, enabling the acquisition of 3D images well representative of AuNPs course within the cells environment. Particularly, the reported methodology makes use of a simple and convergent approach that allows straightforward coating of PEG and fluorescent oligoaziridine oligomers onto the AuNPs surface. The incorporation of a fluorescent oligoaziridine layer avoids major fluorescence self-quenching, the major limitation of AuNPs fluorescent tagging. Furthermore, the PEG layer confers not only the desired stability, but also a higher cellular internalization. We envisage that biotags tethering with specific antibodies or peptide sequences will be capable of selectively target cancer cells. Additional conjugation of these formulations with anti-cancer drugs will permit their use in cancer therapy. Such features, allied to powerful tools such as photothermal microscopy, fluorescence microscopy and cancer imaging make these biotags, especially Au-MPM-OA, valuable tools for biotagging and cancer theragnosis.

4. Experimental Procedures

4.1 Materials

A549 non-small lung carcinoma cell line was purchased from ATCC (Middlesex, UK). Sodium azide was acquired from Amresco (Solon, OH, USA). Fetal bovine serum (FBS) was purchased from Biochrom AG (Berlin, Germany). Tris Base was obtained from Fisher Scientific (Lisbon, Portugal). CellLight® Actin-GFP, BacMam 2.0 (GPF) was attained from Invitrogen, Life Technologies (Madrid, Spain). Glass bottom dishes were dispensed by MatTek Corporation (Ashland, MA, USA). Maleimide-PEG-Maleimide (MPM, Mw= 3.4 Da) was bought from NANOCS (New York, NY, USA). Amphotericin B, collagen solution, ethanol (EtOH), glutaraldehyde, Ham's Nutrient Mixture-F12, L-glutamine, penicillin G, phosphate-buffered saline (PBS), streptomycin, tetrachloroauric (III) acid ($HAuCl_4.3H_2O$), 3-(4,5-dimethylthiazol-2-yl)-5-(3-carboxymethoxyphenyl)-2-(4-sulfophenyl)-2H-tetrazolium reagent MTS, trisodium citrate and trypsin were purchased from Sigma Aldrich (Sintra, Portugal). The oligoaziridine biosensor (OA) was synthesized as described elsewhere.[24]

4.2 Methods

4.2.1. Synthesis of gold nanoparticles

The synthesis followed the Frens method.[31] Briefly, 100 ml of 0.01% (w/v) $HAuCl_4.3H_2O$ were heated until reflux. Then, 1mL of trisodium citrate hydrate, 1% (w/v) was added to the refluxing solution under constant stirring. After 25 sec, the slightly yellow solution turned faintly blue. Subsequently, the solution color changed to dark red, which was indicative of the

formation of monodisperse spherical particles. The solution was boiled for more 5 min to allow the complete reduction of the gold chloride. The AuNPs obtained were then supplemented with 0.05% (w/v) sodium azide and stored at 4°C. Gold nanoparticles produced by this method are referred as AuNPs. UV-Vis: λmax= 525 nm. IR (film) ν (cm^{-1}): 1575 (C=O), 1393 (COO), 1078 (C–O).

4.2.2. Coating of gold nanoparticles with the oligoaziridine biosensor

Different molar ratios of oligoaziridine (100:1, 500:1, 750:1, 1250:1, 2500:1, 5000:1) were added to the colloidal solution of AuNPs and vortexed at low speed, during 2 min. The samples were then ultracentrifuged at 14500 x g, during 20 min, at room temperature. The supernatant was then removed and the pellet was redispersed in deionized water for all the subsequent tests. The nanoparticles produced by this method are denoted as Au-OA. Oligoaziridine biosensor: UV-Vis: λmax= 370 nm. IR (film) ν (cm^{-1}): 1658 (C=C), 1362 (S=O), 1156 (S=O), 1038. Au-OA biotag: UV-Vis: λmax= 525 nm. IR (film) ν (cm^{-1}): 1650 (C=C), 1362 (S=O), 1148 cm^{-1} (S=O), 1030, 1077.

4.2.3. Coating of gold nanoparticles with homobifunctional maleimide poly(ethylene) glycol

The AuNPs produced according to the Frens method were capped with MPM and are denoted as Au-MPM. Different ratios of MPM (PEG:AuNPs) (500:1, 750:1, 1250:1, 2500:1, 5000:1, 10000:1) were added to 10 mL of AuNPs colloidal solution. The mixture was allowed to react for one hour under stirring.[28] Afterwards, the reaction mixture was collected to 1.5 mL eppendorfs and centrifuged at 13500 x g, for 20 min at room temperature. The supernatant was removed and the pellet was redispersed in Tris buffer (pH 7.4) and stored at 4°C, until further use. Au-MPM biotag: UV-Vis: λmax= 525 nm; IR (film) ν (cm^{-1}): 1629 (C=O), 1552 (COO), 1296 (C–N), 1137 (C–O–C); 1050, 1036.

4.2.4. Coating of Au-MPM with oligoaziridine biosensor

The oligoaziridine biosensor was also added to Au-MPM and the samples were ultracentrifuged using the protocol above described. The samples were then re-suspended in water and, again, different molar ratios of OA biosensor were added (100:1, 500:1, 750:1, 1250:1, 2500:1, 5000:1). The mixtures were stirred during 1h in the dark and then re-centrifuged at 13500 x g, for 20 min. The supernatant was removed and the pellet was redispersed in deionized water for subsequent analyses. The nanoparticles produced with this procedure are designated by Au-MPM-OA biotag. UV-Vis: λmax= 525 nm. IR (film) ν (cm^{-1}): 1650 (C=C), 1635 (C=O), 1362 (S=O), 1148 (S=O); 1030, 1077.

4.2.5. Biotags properties and characterization

The morphology of the nanoparticles was analyzed by TEM. Samples were visualized and recorded using Hitachi H8100 TEM itch ThermoNoran light elements EDS detector and digital image acquisition. Nanoparticle's size was determined by dynamic light scattering (DLS). Briefly, nanoparticles were diluted in 800 µL of ultrapure water. [32] Size measurements were then performed in a nano partica SZ-100 series instrument from Horiba scientific, in automatic mode and with a scattered light detection angle of 90°. Zeta potential quantification was carried out in the same nano partica SZ-100 series Horiba instrument using a zeta dip cell with a scattered light detection angle of 173°. Thermogravimetric analysis was performed on a TGA-DSC–STA 449 F3. Samples, previously lyophilized, were placed in platinum sample pans and heated under an argon atmosphere at a rate of 10 °C/min to 700 °C .[35]

4.2.6. Biotags spectral properties

FTIR spectra were recorded in a Nicoletis 20 spectrophotometer (64 scans) from Thermo Scientific equipped with a Smart iTR auxiliary module. Fluorimetry assays were performed in a Perkinelmer LS 45 Luminescence Spectrometer. UV-Vis spectroscopy was recorded in an Infinite 200 from Tecan using a Corning 384 Flat Bottom Black Polystyrene Low Volume/Flat microplate, kindly provided by Corning Corporation. The test was performed in a scan method from 260 to 700 nm.

4.2.7. Cell culture and biotags transfection

Cell culture experiments were performed using of A549 cell line. Cells were cultured in Ham's Nutrient Mixture-F12 medium supplemented with 10% v/v heat-inactivated FBS and antibiotic-antimycotic (penincilin G (100 U/mL)), spectromycin G (100µg/mL) at 37°C, under 5% CO_2 humidified atmosphere. In vitro transfection studies were carried out by seeding cells in glass bottom dishes, dispensed by MatTek Corporation (Ashland, USA), at a density of $12x10^3$ cells per well, with 1 mL of Ham's F12K medium supplemented with 10% FBS without antibiotic for 24 h.[2] Nanoparticles were lyophilized, sterilized, resuspended in Ham's F12K medium (2mg/mL) and filtered with a syringe and a filter with a membrane pore of 200 nm, before being added to the cells. Cell's transfection with all types of nanoparticles herein produced was performed and was stopped over 4 h, by exchanging the culture medium by a complete Ham's F12K medium. Subsequently, cell growth was monitored using an Olympus CX14 inverted light microscope (Tokyo, Japan) equipped with an Olympus SP-500 UZ digital camera. This last procedure was repeated for 2 days (see Fig. ESI 4 in Supporting Information).

4.2.8. Fluorescence and Confocal Laser Scanning Microscopy

In order to evaluate the ability of nanoparticles to enter into the cells environment without losing their electronic properties, both fluorescence and confocal laser microscopy assays were performed after in vitro transfection. First, the glass bottom dishes containing transfected live cells were visualized using a Zeiss AX10 microscope (Carl Zeiss SMT Inc., USA) and analyzed with Axio Vision Real 4.6 software. Formerly, the cells cytoplasm was marked with CellLight® Actin-GFP, BacMam 2.0 (GPF), and then, confocal images were obtained with a Zeiss LSM 710 laser scanning confocal microscope (Carl Zeiss SMT Inc. USA) equipped with a plane-apocromat 40x/DIC objective. Data analysis of CLSM images was performed with Zeiss software (Axio Vs40 V4.5) and Imaris Bitplane (Vs7.6.1, Bitplane, Zurich, Switzerland).

4.2.9. Evaluation of the biotags cytotoxic profile

An MTS assay was performed to evaluate nanoparticles biocompatibility according to the manufacturer instructions. Twenty four hours prior to the experiment the cells were seeded at a density of $12x10^3$ cells per well into 96-well plates with 200 µL of cell culture medium supplemented with 10% FBS, without antibiotics. The cells were then incubated with nanoparticles formulations for 24 and 48 hours. All the formulations of nanoparticles were resuspended in pre-warmed culture medium containing 10% FBS and then added to each well. A total of three replicates were considered for each formulation. The absorbance of the samples was measured at 492 nm using a microplate reader Anthos 2010 (Biochrom, UK). Wells containing cells in the culture medium without materials were used as negative control. EtOH 96% was added to wells containing cells as a positive control.[24]

Acknowledgements

We acknowledge LabRMN at FCT/UNL and Rede Nacional de RMN for access to the facilities. Rede Nacional is supported with funds from Fundação para a Ciência e a Tecnologia (FC&T, Lisbon), Projecto de Re-equipamento Científico, Portugal. We thank the financial support from FC&T through Strategic Project PEst-C/EQB/LA0006/2013 and Projects PTDC/EBB-BIO/114320/2009; SFRH/BD/51584/2011. The MIT-Portugal Program (Bioengineering Systems Focus Area) is also acknowledged.

Notes and references

a REQUIMTE, Departamento de Química, Faculdade de Ciências e Tecnologia, Universidade Nova de Lisboa, Campus de Caparica, 2829-516 Caparica, Portugal. *air@fct.unl.pt

b CICS-UBI, Health Sciences Research Center, Faculdade de Ciências da Saúde, Universidade da Beira Interior, Av. Infante D. Henrique, 6200-506 Covilhã, Portugal.

c Instituto de Telecomunicações, Instituto Superior Técnico, Av. Rovisco Pais, 1049-001 Lisboa, Portugal. * vasco.bonifacio@tecnico.ulisboa.pt

1. A. G. Tkachenko, H. Xie, D. Coleman, W. Glomm, J. Ryan, M. F. Anderson, S. Franzen and D. L. Feldheim, *J. Am. Chem. Soc.*, 2003, **125**, 4700–4701.

2. V. M. Gaspar, I. J. Correia, A. Sousa, F. Silva, C. M. Paquete, J. a Queiroz and F. Sousa, *J. Control. Release*, 2011, **156**, 212–222.

3. K. Cho, X. Wang, S. Nie, Z. G. Chen and D. M. Shin, *Clin. Cancer Res.*, 2008, **14**, 1310–1316.

4. R. B. Restani, P. I. Morgado, M. P. Ribeiro, I. J. Correia, A. Aguiar-Ricardo and V. D. B. Bonifácio, *Angew. Chem. Int. Ed. Engl.*, 2012, **51**, 5162–5165.

5. R. B. Restani, J. Conde, P. V. Baptista, M. T. Cidade, A. M. Bragança, J. Morgado, I. J. Correia, A. Aguiar-Ricardo and V. D. B. Bonifácio, *RSC Adv.*, 2014, **4**, 54872–54878.

6. X. Zhang, M. Liu, B. Yang, X. Zhang and Y. Wei, *Colloids Surf. B. Biointerfaces*, 2013, **112**, 81–86.

7. X. Zhang, X. Zhang, L. Tao, Z. Chi, J. Xu and Y. Wei, *J. Mater. Chem. B*, 2014, **2**, 4398-4414.

8. X. Zhang, M. Liu, B. Yang, X. Zhang, Z. Chi, S. Liu, J. Xu and Y. Wei, *Polym. Chem.*, 2013, **4**, 5060-5064.

9. X. Zhang, X. Zhang, S. Wang, M. Liu, L. Tao and Y. Wei, *Nanoscale*, 2013, **5**, 147–150.

10. K. Yamamoto, Z. An, N. Saito and M. Yamaguchi, *Chemistry*, 2013, **19**, 10580–10588.

11. J. Conde, F. Tian, Y. Hernández, C. Bao, D. Cui, K.-P. Janssen, M. R. Ibarra, P. V Baptista, T. Stoeger and J. M. de la Fuente, *Biomaterials*, 2013, **34**, 7744–7753.

12. P. Eaton, G. Doria, E. Pereira, P. V. Baptista and R. Franco, *IEEE Trans. Nanobioscience*, 2007, **6**, 282–288.

13. J. Conde, J. Rosa, J. M. de la Fuente and P. V Baptista, *Biomaterials*, 2013, **34**, 2516–2523.

14. A. H. Faraji and P. Wipf, *Bioorg. Med. Chem.*, 2009, **17**, 2950–2962.

15. N. Khlebtsov and L. Dykman, *Chem. Soc. Rev.*, 2011, **40**, 1647–1671.

16. G. Qiao, Y. Gao, N. Li, Z. Yu, L. Zhuo and B. Tang, *Chemistry*, 2011, **17**, 11210–11215.

17. T. C. Yih and M. Al-Fandi, *J. Cell. Biochem.*, 2006, **97**, 1184–1190.

18. D. a Giljohann, D. S. Seferos, W. L. Daniel, M. D. Massich, P. C. Patel and C. a Mirkin, *Angew. Chem. Int. Ed. Engl.*, 2010, **49**, 3280–3294.

19. J. Zhao, B. Bo, Y.-M. Yin and G.-X. Li, *Nano Life*, 2011, **02,** 1230008-1230019.

20. A. Llevot and D. Astruc, *Chem. Soc. Rev.*, 2012, **41**, 242–257.

21. D. Solis, W.-S. Chang, B. P. Khanal, K. Bao, P. Nordlander, E. R. Zubarev and S. Link, *Nano Lett.*, 2010, **10**, 3482–3285.

22. L. Surface, A. Paul, D. Solis, K. Bao, W. Chang, S. Nauert, L. Vidgerman, E. R. Zubarev, P. Nordlander, S. Link and P. E. T. Al, 2012, 8105–8113.

23. K. a Kang, J. Wang, J. B. Jasinski and S. Achilefu, *J. Nanobiotechnology*, 2011, **9**, 16–25.

24. V. P. Raje, P. I. Morgado, M. P. Ribeiro, I. J. Correia, V. D. B. Bonifácio, P. S. Branco and A. Aguiar-Ricardo, *Biosens. Bioelectron.*, 2013, **39**, 64–69.

25. P. Gobbi and M. S. Workentin, *Langmuir*, 2012, **28**, 12357–12363.

26. E. Oh, K. Susumu, J. B. Blanco-Canosa, I. L. Medintz, P. E. Dawson and H. Mattoussi, *Small*, 2010, **6**, 1273–1278.

27. K. D. Hartlen, H. Ismaili, J. Zhu and M. S. Workentin, 2012, **28**, 864–871.

28. J. Zhu, C. Waengler, R. B. Lennox and R. Schirrmacher, *Langmuir*, 2012, **28**, 5508–5512.

29. J. Ciesielski, D. Lebœuf, H. a Stern and A. J. Frontier, *Adv. Synth. Catal.*, 2013, **355**, 2077–2082.

30. Y. Liu, M. K. Shipton, J. Ryan, E. D. Kaufman, S. Franzen and D. L. Feldheim, *Anal. Chem.*, 2007, **79**, 2221–2229.

31. G. Frens, *Nat. Phys. Sci.*, 1973, **241**, 20–22.

32. V. M. Gaspar, J. G. Marques, F. Sousa, R. O. Louro, J. a Queiroz and I. J. Correia, *Nanotechnology*, 2013, **24**, 275101.

33. R. R. Arvizo, S. Rana, O. R. Miranda, R. Bhattacharya, V. M. Rotello and P. Mukherjee, *Nanomedicine*, 2011, **7**, 580–587.

34. B. Kang, M. a Mackey and M. a El-Sayed, *J. Am. Chem. Soc.*, 2010, **132**, 1517–1519.

35. S. Khatua, P. Manna, W. Chang, A. Tcherniak, E. Friedlander, E. R. Zubarev and S. Link, 2010, 1–10.

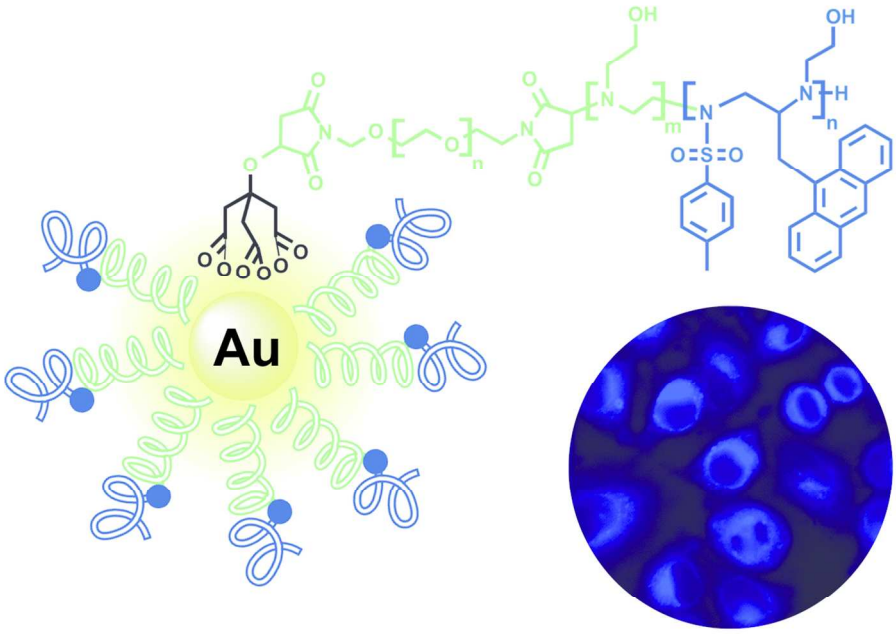

123x92mm (300 x 300 DPI)